Available online at www.sciencedirect.com

ScienceDirect

journal homepage: www.elsevier.com/locate/he

Hydrogen from industrial aluminium scraps: Hydrolysis under various conditions, modelling of pH behaviour and analysis of reaction by-product

Marius Urbonavicius [a,*], *Sarunas Varnagiris* [a], *Ansis Mezulis* [b], *Peteris Lesnicenoks* [b], *Ainars Knoks* [b], *Christiaan Richter* [c], *Darius Milcius* [a], *Rauan Meirbekova* [d], *Gudmundur Gunnarsson* [d], *Janis Kleperis* [b]

[a] *Center for Hydrogen Energy Technologies, Lithuanian Energy Institute, 3 Breslaujos, 44403 Kaunas, Lithuania*
[b] *Institute of Solid State Physics University of Latvia, Riga, Latvia*
[c] *Faculty of Industrial Engineering, Mechanical Engineering and Computer Science, University of Iceland, Reykjavik, Iceland*
[d] *IceTec, Reykjavik, Iceland*

HIGHLIGHTS

- Industrial Al waste utilized for H_2 generation and by-product production.
- Testing impact - NaOH amount, solution and Al amount, temperature on H_2 yield.
- Thermal insulation improved Al-water reaction kinetics in the reactor.
- Simultaneous pH, hydrogen yield, and temperature measurements were conducted.
- A comparison was made between the measured and forecasted pH values by models.

GRAPHICAL ABSTRACT

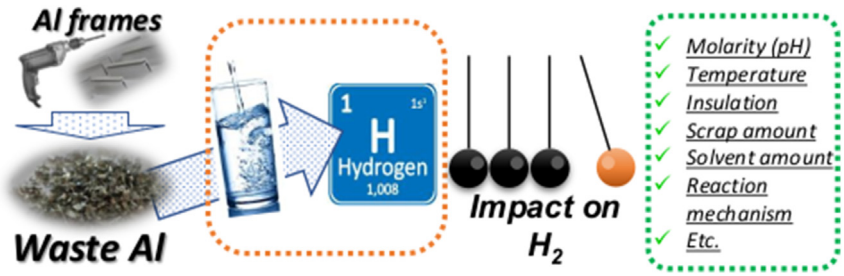

ARTICLE INFO

Article history:
Received 16 June 2023
Received in revised form
18 August 2023

ABSTRACT

The study explores the feasibility of utilizing aluminium scrap waste from the construction industry for hydrogen production via hydrolysis. Specifically, the study involves a primary analysis of aluminium scrap waste and the impact of various reaction parameters, such as NaOH molarity, reaction temperature, amount of Al scrap, solvent quantity, and the reaction vessel insulation, and their effects on the reaction rate, H_2 yield, and by-product

* *Corresponding author.*
E-mail addresses: marius.urbonavicius@lei.lt (M. Urbonavicius), sarunas.varnagiris@lei.lt (S. Varnagiris), ansis.mezulis@gmail.com (A. Mezulis), peterisl@cfi.lu.lv (P. Lesnicenoks), ainars.knoks@cfi.lu.lv (A. Knoks), cpr@hi.is (C. Richter), darius.milcius@lei.lt (D. Milcius), rauan@taeknisetur.is (R. Meirbekova), gudmundur@taeknisetur.is (G. Gunnarsson), janis.kleperis@cfi.lu.lv (J. Kleperis).
https://doi.org/10.1016/j.ijhydene.2023.09.065

Please cite this article as: Urbonavicius M et al., Hydrogen from industrial aluminium scraps: Hydrolysis under various conditions, modelling of pH behaviour and analysis of reaction by-product, International Journal of Hydrogen Energy, https://doi.org/10.1016/j.ijhydene.2023.09.065

Accepted 7 September 2023
Available online xxx

Keywords:
Hydrogen generation
Hydrolysis
Waste aluminium
Arrhenius calculation
Alkali solution
pH modelling

formation. The pH of the reaction solution was continuously monitored to determine the reaction mechanism, while the structure of the by-product was analysed at two stages: after removal and drying, and after removal and washing. Our findings indicate that increasing the reaction temperature has the most significant influence on the reaction kinetics. Insulating the reaction vessel ensured self-promoted hydrogen production due to the heat generated from the exothermic reaction inside the vessel, resulting in an approximate temperature increase of 5 °C for all tested reaction solution molarities compared to non-insulated conditions. The pH measurements were conducted in two different ways. The first one involved immersing a pH probe directly into an open reaction container. The second approach utilized a closed reaction container under isothermal conditions, where both the pH and H_2 yield were measured simultaneously. In addition, the obtained data was compared between the measured pH values and the predictions generated by models utilizing the measured H_2 evolution in order to forecast the pH behaviour. The modelling results recognize and suggest the existence of separate reaction phases or zones, each characterized by distinct influences on the pH level.

1. Introduction

The last decade, and especially the current time is an outstanding period as we are facing various issues in terms of climate change, global warming, energy crisis and so on. Among others, waste generation and sustainable management are recognized as a growing challenges for the welfare of our planet and mankind [1,2]. According to previous articles, the generation of global municipal solid waste reached several billion metric tonnes during the last years and it is foreseen to rise to about 3.4 billion by 2050 [3–6]. Proper waste management must be ensured in order to avoid environmental pollution and public health hazards, which could be caused by open dumping, landfilling, disposal into water or other unsustainable waste disposal activities. Therefore, the implementation of a true circular economy with various other alternatives for cleaner waste management is encouraged including reuse, recycle, repurpose, energy recovery, etc. [7,8].

Meanwhile, increasing aluminium (Al) demand as a strategic material in Europe (estimated 40% increase in demand by 2050) suggests increased aluminium waste generation. Consequently the recycling of Al is considered to be a key to sustainable circular economic development [9,10]. Although Europe is one of the world leaders in Al recycling industry, huge amounts of Al currently is still landfilled or wasted. Therefore, innovative improvements that increase sustainable waste management of Al waste is highly desirable. New ways to utilize or recycle Al waste have to be developed in order to reduce landfilled or unused Al waste, which pollutes ground, rivers, and streets as well as poses a danger of combustion via reaction with water and hydrogen production. But the posed danger can be turned into a feature not a bug, as a low-value waste Al can be utilized for energy generation on-demand. The concept of waste-to-hydrogen is recognized as an attractive solution for generating a zero-carbon fuel from waste material [11–13].

Specifically, waste aluminium can be used during the hydrolysis process, where aluminium particles react with water to produce zero-carbon hydrogen. The hydrolysis of aluminium is known as an efficient, inexpensive and environmentally friendly way to produce hydrogen [14,15]. Such produced hydrogen is highly pure and therefore can be applied directly for production of electricity via fuel cells or decarbonization of combustion fuels such as use in an internal combustion engine or gas turbines [16–18]. In comparison to catalyst enhanced hydrogen production (for example methane steam reforming) which require ample amounts of energy, time and resources [19] or suggested storage in hydride forms [20] the Al water reaction provides a cost effective solution for sustainable hydrogen supply and storage.

During this reaction up to 11% of hydrogen mass compared to the weight of aluminium can be generated, which, in most cases, is higher than the commonly used storage methods of hydrogen. Under ambient conditions, theoretically, the reaction of 1 g of aluminium with water can yield 1.36 L of hydrogen gas [21]. Therefore this reaction is an important way to initiate H_2 generation on-demand [22]. Additionally, due to the exothermic origin of the reaction, 4.3 kWh of heat per kg aluminium is co-produced with the hydrogen. The solid by-product of the process is mainly $Al(OH)_3$; there are potential application for this side-product aluminium hydroxide which could make this option for scrap aluminium recycling or energy recovery even more sustainable and economical [23]. Considering that the aluminium itself is the most abundant metal in the earth's crust, which has a very high energy density. It is an environmentally safe and relatively cheap metal with an oxidation state of +3, contributing to better hydrogen production as compared to other active metals [24,25]. On the other hand, the increasing demand for the utilization of clean energy sources leads towards to the pursuit of innovative technologies. In this case, hydrogen is considered as a “hot topic” in the modern energy world. It is recognized as an ideal

Please cite this article as: Urbonavicius M et al., Hydrogen from industrial aluminium scraps: Hydrolysis under various conditions, modelling of pH behaviour and analysis of reaction by-product, International Journal of Hydrogen Energy, https://doi.org/10.1016/j.ijhydene.2023.09.065

future (and in some cases today's) energy source due to the high energy content (approximately thrice of the gasoline) which does not generate any harmful pollutants during the process of energy generation [12,26,27]. Because of these, and other characteristics, hydrogen is presented as one of the best alternatives to tackle the climate change and energy crisis.

There are various articles which look at waste aluminium utilization for hydrogen production using different modifications of hydrolysis reaction. For instance, S. P. Tekade et al. used waste aluminium metal wire to generate hydrogen from human urine in the presence of liquid metal gallium (Ga) and sodium hydroxide (NaOH) [12]. Other scientists examined waste aluminium cans in low alkaline aqueous solution, where Al cans were pre-treated using various ball milling combinations as well as hand grind. Before the ball milling, the paint was removed in concentrated sulfuric acid. Moreover, during the hydrogen generation, Ni or Ni/Bi additives were used for better H_2 yield [28]. S. T. Lim et al. used waste aluminium cans in powdered form together with other metallic powdered additives, such as Sn, Zn or Mg. They showed that binary composite (powdered Al cans with 3% Sn) has the highest H_2 yield [29]. Other authors present their results where waste Al of soda rings was used with a solution of sodium hydroxide from 1 M to 10 M [30]. In all aforementioned cases, some technical and fundamental questions still need to be answered, such as reaction mechanism is not clear; at large concentrations, the hydroxide poses a hazard, and the makeup is unclear; pre-treatment or additives introduce complexity into the system.

The increment of the amount of sodium hydroxide in the aluminium water reaction is a simple and effective way to increase H_2 yield. Still, as it can be seen from the other authors work, the majority of them use additives or other pre-treatment methods in order to successfully employ waste aluminium for H_2 production [31–37]. These strategies are appropriate for scientific experiments, but talking about the industry, any additional steps, such as ball milling, introduction of Ga, etc. consume time, materials, and other resources. Therefore, the commercial application of aluminium reaction with water for hydrogen production is very limited in the industry sector. It appears that the cost of these mechanical and chemical pre-treatments may mean that economically viable hydrogen production from aluminium scrap might, at least currently, only be possible with relatively pure aluminium waste with micron-level or even smaller particle dimension. In addition, it is not clear how initial parameters influence the by-product, as recycling/reusing $Al(OH)_3$ is crucial step for true circular economy and green hydrogen.

In the present work, we examine the possibility of using aluminium scrap from the construction industry for hydrogen production by hydrolysis. Specifically, aluminium scraps were received directly from the drilling process of aluminium profiles, which in this case are used to fabricate insulating glass windows frames, doors, etc. To our knowledge this is the first analysis of the suitability and performance of this very widely encountered type of construction sector Al waste for the hydrolysis process. The analysis of such waste Al is reasonable because even a small aluminium construction company can produce tens of kilograms of such waste per day. A series of experiments were performed including different NaOH molarity, reaction temperature, amount of Al scrap, insulation or non-insulation of the reaction vessel, etc. Also, the results include the calculation of the Arrhenius equation constant. Moreover, the analysis and modelling of the reaction mechanism (basically pH behaviour during the Al-water reaction) and reagent structure were performed as well to better understand the formation process of the reaction by-product.

2. Materials and methods

2.1. Materials

Waste aluminium scraps were received from company "Stiklita, JSC". Stiklita produces aluminium frames for insulating glass units and other household application. As-received aluminium scrap was used during all the hydrolysis reaction without any additional pre-treatment. NaOH (>99% purity) pellets were used for the preparation of an alkali solution. Distilled water was used as a base for the alkali solution. After the hydrolysis reaction, the solution, which consists of alkali and reacted waste Al material, was poured out into a Petri dish and left in an ambient atmosphere at room temperature until the water evaporated. The obtained sediments were extracted from the Petri dish and designated as the solid reaction by-product. Another batch of by-product was washed after pouring out into a Petri dish.

2.2. Hydrolysis reaction

A custom-made laboratory stand was used for hydrogen generation by reacting waste Al scrap with the alkali solution (0.24, 0.5 and 1 M). Fig. 1 is a schematic of the reactor system. The main components were: i) *Reaction flask*. For measuring of reaction temperature, some experiments were performed with an in-flask thermocouple with the reaction flask fully wrapped with thermal-insulation material made from polystyrene; ii) *A water bath for temperature control*, used to control

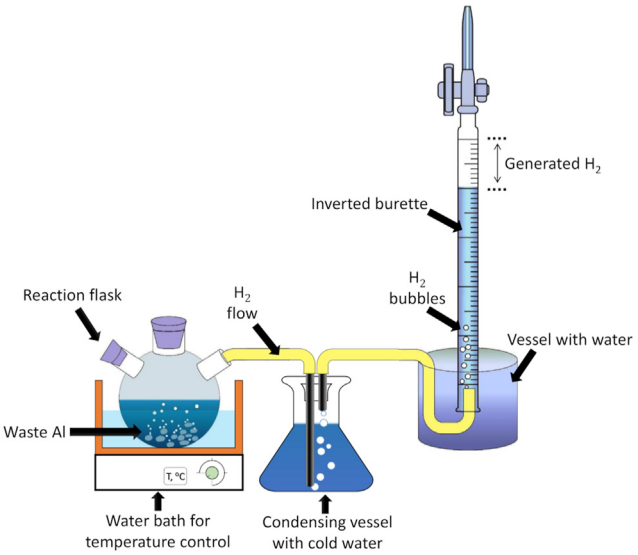

Fig. 1 – Hydrogen production reaction scheme.

Please cite this article as: Urbonavicius M et al., Hydrogen from industrial aluminium scraps: Hydrolysis under various conditions, modelling of pH behaviour and analysis of reaction by-product, International Journal of Hydrogen Energy, https://doi.org/10.1016/j.ijhydene.2023.09.065

or limit the reaction flask temperature in the range of 20–70 °C; iii) *Interim flask with cold water*. This flask was used as condensing vessel to remove water moisture from the H_2 product stream prior to H_2 measurement, especially needed when the reaction temperature was allowed to rise to above 40 °C; iv) *Inverted burette*, which was used for quantifying hydrogen production yield. The inverted burette has a graduated scale in steps of 1 mL and filled up with water. The amount of H_2 produced was evaluated by the decrease of water level in the burette. The H_2 generation reaction rate was measured by integrating the H_2 flow with time. The initial conditions were at 20 °C (293.15 K) and 1 atm (101.325 kPa) and experimentally controlled temperature in the range of 20–70 °C.

Various parameters have been analysed in order to evaluate their influence on H_2 production yield via waste Al reaction with alkali solution: the amount of alkali solution, molarity, primary reaction temperature at different molarity, insulation of reaction flask and its influence on reaction temperature.

2.3. Characterization of aluminium scrap

The surface morphology of initial waste Al materials was investigated by scanning electron microscope (SEM, Hitachi S3400 N). The bulk elemental composition and elemental mapping were analysed by energy dispersive X-ray spectroscopy (EDS, Bruker Quad 5040). The initial waste Al was identified by X-ray diffractometer (XRD, Brucker D8) using a Cu Kα radiation and Lynx Eye linear position sensitive detector at 2 theta angles in the range 20–70°. The TOPAS software was used for crystallite size calculation.

2.4. pH and molarity measurements of the alkaline solution

The pH measurements were conducted using the pH/mV meter Metria M21. The pH meter was recalibrated after each measurement using 3-point calibration (pH 4, 7, and 10 buffers). The electrolyte solution with molar concentrations of 0.24, 0.5, and 1 was used to initiate the Al-water reaction. Before the reaction, the pH sensor was immersed in the alkaline solution until it reached pH equilibrium. Two sets of experiments were conducted: one involved measuring pH in an open reaction vessel without considering the temperature impact, while the other involved measuring pH in a closed reaction vessel to maintain isothermal conditions and prevent the solution from coming into contact with air. The sensor was continuously present throughout the entire reaction, and pH readings were recorded at regular intervals throughout the reaction. The pH values were converted to molarity using standard calculations to determine the changes in molarity during the reaction.

2.5. Activation energy

Activation energy is used to assess the energy required for a chemical reaction. Depending on the temperature, the fraction of molecules with energy equal to, or greater than, the activation energy E_a is given by the Arrhenius equation:

$$K = Ae^{-\frac{E_a}{RT}} \quad (1)$$

where K is the reaction rate constant, A – is the frequency factor constant, R – is the universal gas constant, and T – is the absolute temperature. Usually, E_a is derived by performing experiments to determine the reaction rate constant at different temperatures. Taking the natural log of Eq. (1) yields the following:

$$lnK = lnA - \frac{E_a}{RT} \quad (2)$$

Graphing ln K vs. $1/T$ gives a straight line, known as Arrhenius approximation. In this approximation the slope equals $-E_a/R$, and the y-intercept equals ln A.

The activation energy is moderately dependent on particle size and weakly dependent on the alkaline concentration. It is challenging to perform the size separation of Al scrap particles (Fig. 2b). This prevents a simple measurement of the parameters of the particle size distribution, whether Gaussian or otherwise. We therefore defer developing a quantitative model of the kinetics as a function of particle size to future work.

2.6. Characterization of by-products

The BET-specific surface area of the calcined samples was measured with TriStar 3000 surface area and porosity analyser from Micromeritics. The crystal structures of the by-product were analysed using X-ray diffractometer (XRD, Brucker D8) using a Cu Kα radiation and Lynx Eye linear position sensitive detector at 2 theta angles in the range 20–70°.

3. Results and discussion

The comprehensive surface morphology, structure and elemental analysis for waste Al scraps were done by SEM, EDS and XRD techniques. The obtained results are presented in Fig. 2. First of all, it should be mentioned that the waste Al scraps were in dimensions between hundreds of microns to several centimetres, with wide variety of shapes (Fig. 2a and b). Also, the surface morphology measurements revealed that every scrap has two-types of surfaces: one side with straight lines (Fig. 2c), while the other one has waived lines (Fig. 2d). The difference between those surfaces is aimed by drilling process of aluminium profiles. Structural analysis revealed intense aluminium peaks with cubic crystallographic orientation of (111), (200) and (220) at $2\Theta = 38.2°$, 44.5° and 64.9°, respectively (Fig. 2e). Elemental composition showed that waste Al consisted of 94.3 at. % of aluminium, 0.6 at. % of magnesium, 5.0% of carbon and 0.1 at. % of oxygen (inserted table in Fig. 2e). The origin of the surface carbon can be attributed to the metalworking process during the production of aluminium profiles. Meanwhile, magnesium is commonly used material to increase strength, improve corrosion resistance and provide good wettability characteristics to the industrially used aluminium. However, the amount of magnesium is too small to be seen in crystalline form by XRD.

The reactions between the scrap Al and water at different temperatures (20 °C, 30 °C, 40 °C, 50 °C, 60 °C and 70 °C) were

Please cite this article as: Urbonavicius M et al., Hydrogen from industrial aluminium scraps: Hydrolysis under various conditions, modelling of pH behaviour and analysis of reaction by-product, International Journal of Hydrogen Energy, https://doi.org/10.1016/j.ijhydene.2023.09.065

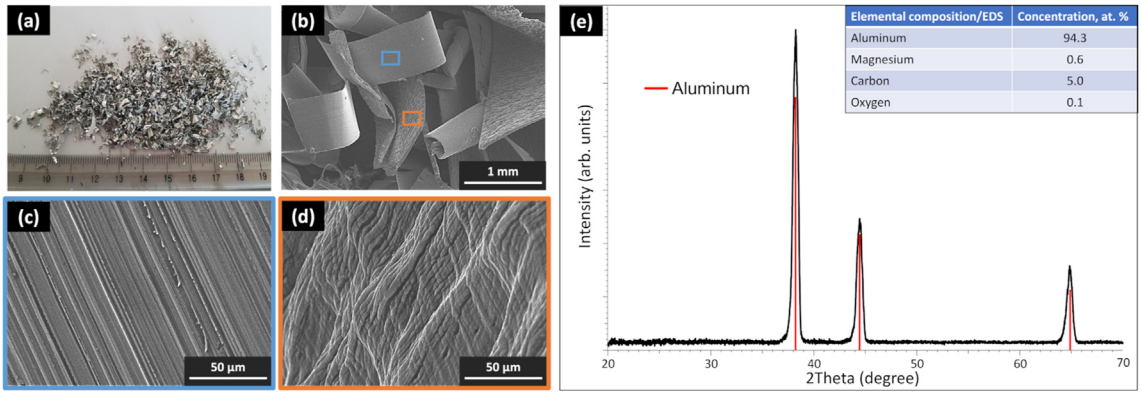

Fig. 2 – (a) Real-image, (b–d) SEM views at different magnitude and (e) XRD graph with inserted EDS elemental composition of initial waste Al scraps.

carried out using different alkali concentrations (0.24 M, 0.5 M and 1 M). Each time, the reaction was carried out using 0.2 g Al scrap and 50 mL alkali solution, and the reaction results are shown in Fig. 3. As the temperature of the 0.24 M alkali solution increased (Fig. 3a), the kinetics of hydrogen generation could be significantly enhanced, while the cumulative change in hydrogen yield was negligible (250 mL of H_2 at 20 °C and 260–270 mL of H_2 at 30–70 °C). The reaction was completed in approximately 140 min at 20 °C, and only in about 30 min at 60 °C and 70 °C.

Similar correlations were observed by increasing the alkali solution to 0.5 M and 1 M, where the hydrogen yield reached about 260 mL (Fig. 3b and c, respectively). In the presence of 0.5 M alkaline solution, the reaction reached completion at 260 mL of H_2 in 173 min (250 mL in 100 min) at 20 °C, and in 70, 24, 18, 9, and 7 min at 30, 40, 50, 60, and 70 °C, respectively. The reaction rate was increased again by increasing the alkali concentration further to 1 M (260 mL of H_2 in 79 min at 20 °C).

In this work we focus on measuring and fitting the reaction rate constant as a function of temperature. We use a well-known chemical reaction model for thin plates [38]. This model distinguishes two reaction regimes: Firstly, conditions where the chemical reaction is the controlling step, secondly, conditions where mass transfer is controlling. In our findings,

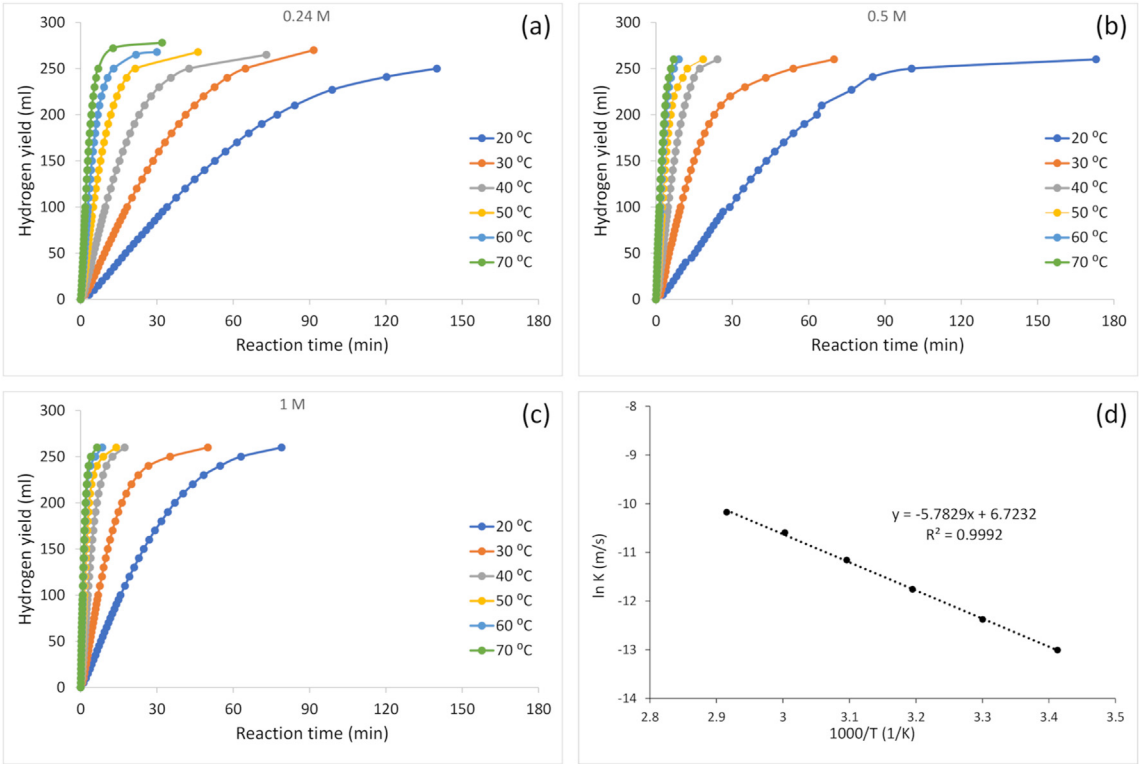

Fig. 3 – Hydrogen production after the reaction between 0.2 g of Al scraps and 50 mL of alkali solution at different temperatures and concentrations: (a) – 0.24 M, (b) – 0.5 M and (c) – 1 M. (d) Arrhenius regression plot and its linear approximation with 0.24 M NaOH solution.

Please cite this article as: Urbonavicius M et al., Hydrogen from industrial aluminium scraps: Hydrolysis under various conditions, modelling of pH behaviour and analysis of reaction by-product, International Journal of Hydrogen Energy, https://doi.org/10.1016/j.ijhydene.2023.09.065

under reported conditions, Al hydrolysis is primarily controlled by chemical reactions. The measured reaction rate fits well across the entire reaction pathway under this assumption (from reaction start to the end).

The key equations of the chemical reaction-controlling model are:

$$X_{Al} = K \times t \tag{3}$$

$$K = \frac{k_i \times c_{OH}^n}{d\rho_{Al}} \tag{4}$$

where X_{Al} is the chemical conversion of aluminium, t is time, k_i is the intrinsic reaction velocity, c_{OH} is alkali concentration, d is the scrap thickness, and ρ_{Al} is aluminium density. As c_{OH} is related to pH measurements, it is preferable to take the decimal log of Eq. (5):

$$\log K = \log \frac{k_i}{d\rho_{Al}} + n \times \log c_{OH} \tag{5}$$

Before the mass transfer effects become important, the value of n is close to unity for every sample and alkali, a finding that suggests that reaction R1 (eq. (6)) may have a rate limiting elementary step that involves a single hydroxyl ion. The Arrhenius plot from 0.24 M NaOH temperature dependent series and obtained values of K are shown in Fig. 3d.

As seen in Fig. 3d, the linear conformity is very good, characterized by the R-squared value of 0.9992. The activation energy, E_a, for this chemical reaction series is consequently determined to be 48.1 kJ/mol.

Comparing different alkali concentrations at the same temperature (Fig. 4a), 250 mL of hydrogen was produced in 140, 100 and 63 min using 0.24, 0.5 and 1 M alkali, respectively. Thus, the reaction time can be reduced by 55% by quadrupling the alkali concentration. However, the kinetics of the reaction appear to be more dependent on the temperature factor, as the reaction delay can be shortened and the rate of hydrogen production increased even more notably by increasing the temperature.

Another factor that can affect the reaction kinetics, and is rarely considered, is the ratio of the volume of alkali solution to metal. In Fig. 4a we used our default ratio of 1 g Al: 250 mL solution. In Fig. 4b we report the effect of varying the metal to solvent ratio. The reactions were performed using 25, 50, 100 and 200 mL alkali solution at room temperature with the fixed amount of 0.2 g Al scrap in each run, i.e. we tested the ratios 1 g Al: 125 mL, 1 g Al: 250 mL, 1 g Al: 500 mL and 1 g Al: 1 L. The reaction started after about 3 min with 25 and 50 mL, and after 1.6 min with 100 and 200 mL of alkali solution, respectively. Moreover, hydrogen production rate was accelerated by increasing the amount of alkali solution from 25 mL (250 mL of H_2 produced in 120 min) to 100 mL (250 mL of H_2 produced in 61 min). A further increase in the volume of the alkali solution to 200 mL did not affect the reaction kinetics and was observed in the same way as in the case of 100 mL.

Presumably, more solution with the same amount of scrap Al means more OH groups are free to move, reach and break down the alumina layer and support the reaction. The reduced amount of water tends to prolong the reaction because the Al scrap occupies a relatively larger volume in the vessel, and the increasing amount of the reaction by-product can also act as a barrier.

Although the type of water (tap water, seawater, pure water) was not considered in this work, it is worth noting that it can also be an important factor in hydrogen production [39].

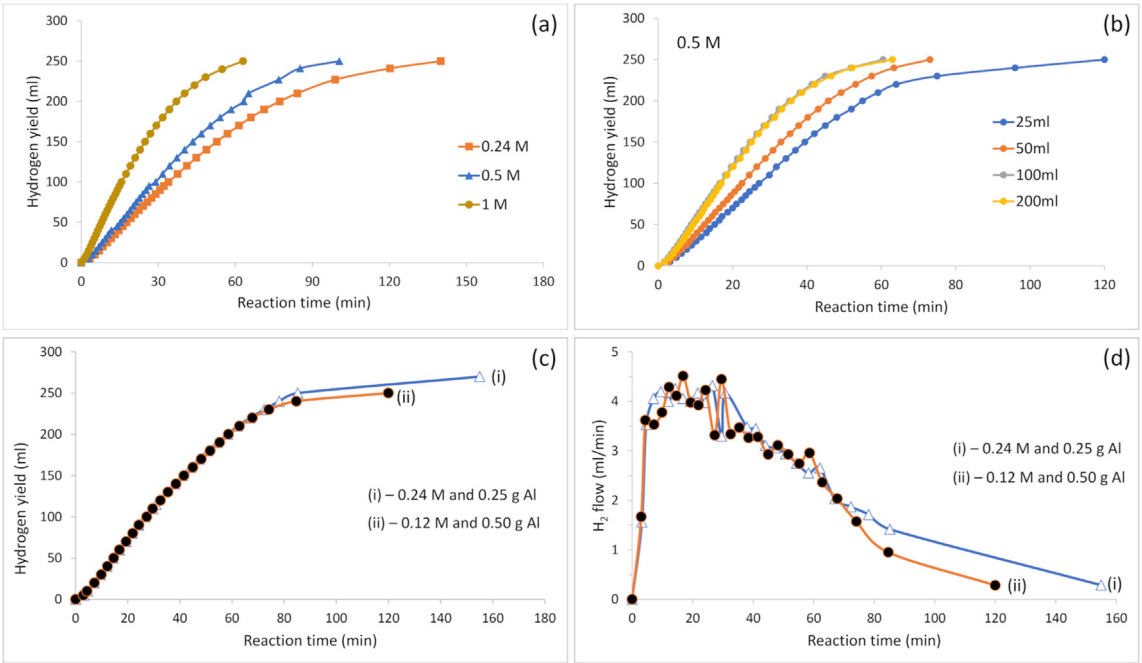

Fig. 4 – Hydrogen production after the reaction between 0.2 g of Al scraps and 50 mL of alkali solution at 20 °C using (a) different alkali concentrations, and (b) varying solution amount with a constant molarity of 0.5 M. (c) Hydrogen production and (d) flow by reaction between (i) 0.25 g of Al scraps with 50 mL of 0.24 M alkali solution and (ii) 0.5 g of Al scraps with 50 mL of 0.12 M alkali solution.

Please cite this article as: Urbonavicius M et al., Hydrogen from industrial aluminium scraps: Hydrolysis under various conditions, modelling of pH behaviour and analysis of reaction by-product, International Journal of Hydrogen Energy, https://doi.org/10.1016/j.ijhydene.2023.09.065

If the hydrogen produced by the hydrolysis reaction were to be used to generate electricity on-board, it may be desirable to assess the impact of the water type, as the surrounding environment may determine the conditions of the used water.

One of the simplest and cheapest ways to break down the passive oxide layer is to use hydroxide promoters (NaOH, KOH, 2.5% wt. H_2 yield) [40]. However, the main challenge in using a highly alkaline solution (e.g., 5 M or more) is its corrosive nature, not only increasing safety requirements on scaling up the technology but also might damage the fuel cell membrane if hydrogen is supplied directly after the reaction to the fuel cell. To reduce the concentration of the alkali solution but ensure the same fast reaction process, the kinetics of hydrogen generation could be controlled by combining the alkali concentration and the mass of Al scrap (Fig. 4c and d). The reaction kinetics were very similar with decreasing alkali concentration from 0.24 M to 0.12 M and increasing the mass of aluminium scrap from 0.25 g to 0.50 g, respectively (Fig. 4d). However, with a higher concentration of alkaline solution, more hydrogen is produced (270 mL) compared to when a lower concentration (250 mL) is used (Fig. 4c). Of course, when more aluminium is used with a lower alkali concentration, there is a high probability that the reaction is incomplete and the final by-product will contain the additives of pure metallic Al.

Aluminium scrap as a low value waste could be utilized to produce both hydrogen and heat in reaction with water that yield 0.11 kg of H_2 and about 15–16 MJ (≈4.3 kWh) of heat per 1 kg of Al [23,41]. First, the reaction was carried out using 0.2 g of Al scrap with 50 mL of different alkali solutions (0.24 M, 0.5 M, and 1 M) in a non-insulated glass vessel with a thermocouple mounted inside to record the temperature data during the reaction (Fig. 5a–c). Each time, the reaction was initiated using room temperature (23 °C) alkaline solution. The maximum temperature reached during the reaction increased with increasing alkali concentration, 26 °C at 0.24 M, 27 °C at 0.5 M, and 29 °C at 1 M, respectively.

In order to achieve the maximum amount of heat dissipated during the reaction, it is necessary to consider not only the thermodynamic and reaction conditions, but also the thermal insulation of the vessel used in the open space. In this case, the same glass vessel was insulated with polystyrene foam and the above-mentioned reactions were repeated (Fig. 5d–f). This time, the temperature peak reached by the reaction increased even more, 30.3 °C at 0.24 M, 32.2 °C at 0.5 M, and 33 °C at 1 M, respectively. It is also interesting to note that the shape of the temperature rise curve almost coincides with the hydrogen production curve. Furthermore, at lower alkali concentrations (Fig. 5d and e), the hydrogen production rate increased and the reaction was completed faster compared to the reaction in the non-insulated vessel (Fig. 5a and b). Therefore, a properly selected reaction vessel can help to ensure self-promoted hydrogen production due to the heat generated during the exothermic reaction inside the vessel.

To gain a deeper understanding of the mechanism behind the aluminium-water reaction, it is crucial to consider the alterations in the pH value of the solution. The leading hypothesis for the mechanism of aluminium hydrolysis and hydrogen evolution in alkaline solutions (pH > 10) is that the high alkalinity results in the de-passivation of the aluminium metal, which in turn allows aluminium hydroxide ions ($Al(OH)_4^-$) to dissolve into solution [42–47]. A possible mechanism for aluminium hydrolysis with hydrogen evolution can then be expressed by the following two 'half reactions' [48–51]:

$$Al[metal] + 4OH^-[aq] \leftrightharpoons 3e^-[metal] + Al(OH)_4^-[aq] \quad (\text{R1} - \text{Al dissolution}) \tag{6}$$

$$3e^-[metal] + 3H_2O \leftrightharpoons 3OH^-[aq] + \frac{3}{2}H_2 \quad (\text{R2} - \text{Water splitting}) \tag{7}$$

Clearly the net process results in a pH downshift, i.e., the net consumption of one hydroxide ion.

This pH downshift should continue until the concentration of aluminium ions, at high pH predominantly the species $Al(OH)_4^-[aq]$, reaches saturation. The saturation threshold is a function of parameters like pH (base molarity) and solution temperature together with the Al ion concentration. Once the saturation point is reached in a given experiment the precipitation of the solid product will commence [42,46]. Although several species can precipitate, namely various aluminium hydroxides or sodium aluminates depending on the solution parameters, the dominant solid precipitate typically aimed for is the precipitation of amorphous, Gibbsite or Bayerite aluminium hydroxide [52]:

$$Al(OH)_4^-[aq] \leftrightharpoons Al(OH)_3[solid] + OH^-[aq] \quad (\text{R3} - \text{Aluminium hydroxide precipitation}) \tag{8}$$

The combination of these reactions (hydrolysis and precipitation) predicts an initial rapid pH downshift that will slow down, or may even reverse into a pH upshift, when the concentration of $Al(OH)_4^-[aq]$ and $OH^-[aq]$ and temperature reach a level where that precipitation of $Al(OH)_3[solid]$ commence.

To investigate the behaviour of pH and reaction progress, a batch of experiments was conducted using different molarities of solution. The pH values were measured in an open reaction container during the reaction between aluminium and an alkaline solution. The changes in pH and molarity of the alkaline solution over time are presented in Fig. 6. The

Please cite this article as: Urbonavicius M et al., Hydrogen from industrial aluminium scraps: Hydrolysis under various conditions, modelling of pH behaviour and analysis of reaction by-product, International Journal of Hydrogen Energy, https://doi.org/10.1016/j.ijhydene.2023.09.065

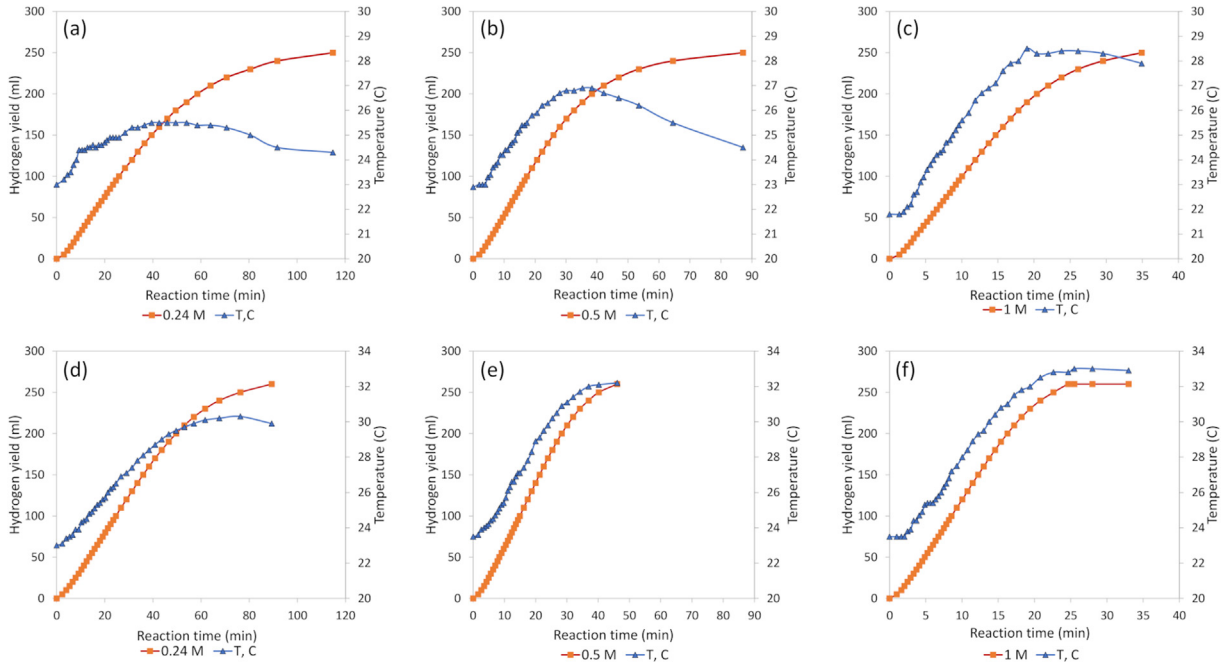

Fig. 5 – Hydrogen production between 0.2 g of Al scrap with 50 mL of alkali solution of different concentrations (a–c) in a non-insulated reaction vessel and (d–f) in a thermally insulated reaction vessel. The hydrogen production curves are marked with orange squares and the temperature curves inside the vessel during the reaction are marked with blue triangles. (For interpretation of the references to colour in this figure legend, the reader is referred to the Web version of this article.)

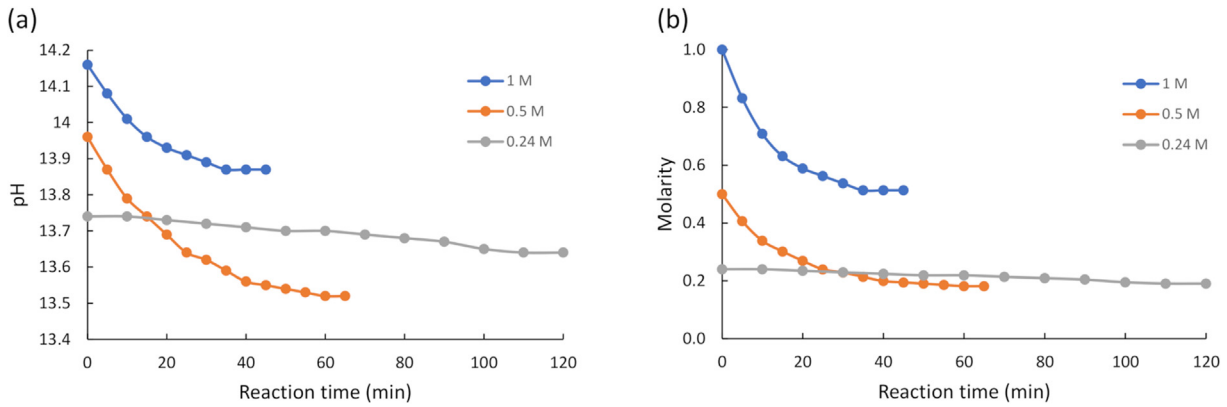

Fig. 6 – Evaluation of electrolyte pH (a) and molarity (b) changes during the aluminium-water reaction in an open vessel.

alkaline solution molarities (0.24 M, 0.5 M and 1 M) corresponds to pH values of 13.74, 13.96 and 14.16, respectively. During the measurement, the pH value changes were recorded every 5 min. The data in Fig. 6 shows an almost linear slow downshift at 0.24 M NaOH, and a very rapid large pH downshift for higher NaOH molarities that levels off quickly. A pH decrease was observed from 13.74 to 13.64 for the reaction initiated at 0.24 M after 120 min of reaction time. In terms of molarity, it is approximately 20.5% decrease comparing the initial and the final molarity values. The other two reactions initiated at 0.5 M and 1 M showed an even more significant decrease in pH values: from 13.96 to 13.52 for 0.5 M (64% of molarity decrease) in 65 min of the reaction time and from 14.16 to 13.87 for 1 M (49% of molarity decrease) in 45 min of the reaction time.

The observed pH and molarity indicate a significant downshift. However, this experiment overlooked the impact of temperature, which can be substantially increased by the exothermic nature of the reaction (as in Fig. 5). The pH is widely recognized to be highly sensitive to the temperature of the measured solution, suggesting that this oversight may have distorted the obtained results to some extent. Furthermore, the use of an open reactor allowed the solution to interact with atmospheric air during its reaction with aluminium. Consequently, it is plausible that the measurements primarily reflected the reaction of NaOH with

Please cite this article as: Urbonavicius M et al., Hydrogen from industrial aluminium scraps: Hydrolysis under various conditions, modelling of pH behaviour and analysis of reaction by-product, International Journal of Hydrogen Energy, https://doi.org/10.1016/j.ijhydene.2023.09.065

atmospheric CO_2, rather than the consumption of OH by aluminium. This explanation may be relevant since the NaOH solution is commonly known to be utilized for CO_2 capture purposes [53].

An increase in temperature can lead to changes in the autoionization constant of water, known as Kw(T), which in turn affects the pH level. Since the main aim of this investigation is to specifically assess the effect of Al dissolution (and concentration of hydroxide ions) on pH, it is scientifically reasonable to maintain an isothermal environment within the reactor enhancing the reliability of the scientific findings. Therefore, another series of experiments was conducted to eliminate the influence of atmospheric air and the temperature variations during exothermic reactions. To maintain nearly isothermal conditions throughout the process, the reaction vessel was placed in a stirring water bath with circulating water. The temperature was set to 20 °C. The hermetic reaction vessel was equipped with a pH meter and temperature probe. Three different experiments were carried out using molarities of 0.24 M, 0.5 M, and 1 M. The amount of produced hydrogen, pH value, and temperature were measured simultaneously, as depicted in Fig. 7. In this case, the deviation of the reaction temperature remained insignificant throughout the entire duration of the reaction.

Interestingly, it is apparent that there is no straightforward relationship between hydrolysis and pH level. At a solution concentration of 0.24 M, the pH consistently decreased (Fig. 7a), while at 0.5 M and 1 M, the pH either increased or remained relatively constant (Fig. 7b and c), despite the significant progression of the H_2 reaction.

The subsequent figures presented below depict a comparison between the measured pH values and the predictions generated by models that employ the measured H_2 evolution to forecast the pH behaviour.

The activity coefficient of hydroxide ions (γ_{OH^-}) plays an important role in understanding the behaviour of aqueous

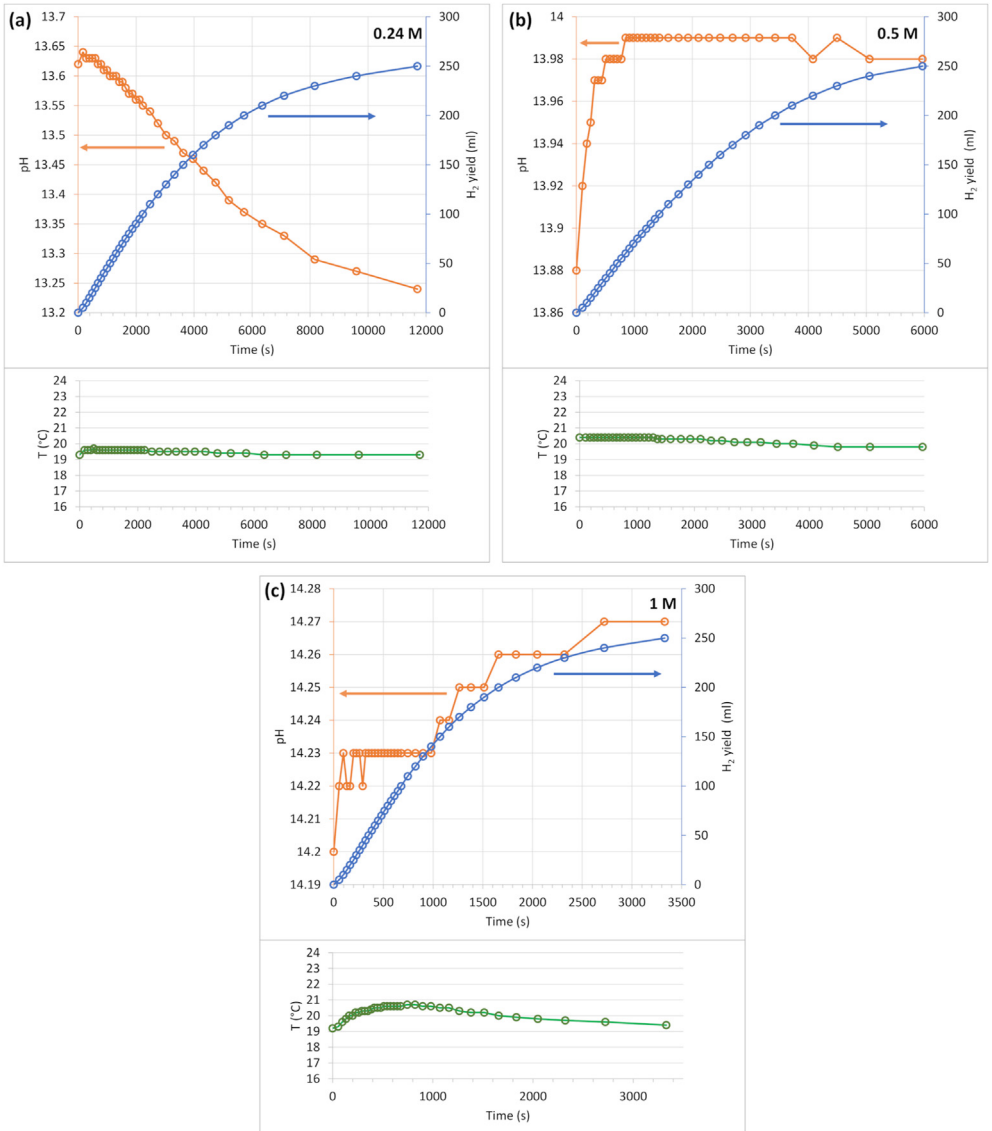

Fig. 7 – Simultaneous measurement of pH, hydrogen yield and temperature conducted in a closed vessel using 0.2 g of aluminium and 50 mL of solution with NaOH molarities of (a) 0.24 M, (b) 0.5 M and (c) 1 M.

Please cite this article as: Urbonavicius M et al., Hydrogen from industrial aluminium scraps: Hydrolysis under various conditions, modelling of pH behaviour and analysis of reaction by-product, International Journal of Hydrogen Energy, https://doi.org/10.1016/j.ijhydene.2023.09.065

solutions and their impact on various chemical processes [54]. It represents the deviation of the ion concentration from their ideal values. It is used to account for the non-ideal nature of the solution and adjust the concentration of hydroxide ions when calculating pH. By incorporating γ_{OH^-} into models, the accuracy of pH predictions can be improved, providing deeper insights into the underlying chemical reactions.

At concentration of 0.24 M NaOH, the best fit model assumes γ_{OH^-} adjust to 1.27 after the introduction of metal ion (compared to measured γ_{OH^-} value of 1.12 prior to the introduction of metal ion) and system H_2 measurement delay of 114 s relative to pH measurement delay (≈0 s). However, even the raw unadjusted pH model (red $\Delta OH^- = -1$ in Fig. 8a), i.e., a model that simply uses a fixed γ_{OH^-} of 1.12 as was measured in the NaOH solution with no metal ions, shows a remarkably good agreement with the measured pH downshift.

A best fit model can be obtained by assuming a reaction path that passes through three zones or phases, albeit that at 0.24 M NaOH the first two phases (pure hydrolysis and transitory precipitation) is almost negligibly short (Fig. 8b). Note that observing these distinct reaction phases or zones becomes more noticeable from a concentration of 0.5 M and higher. To our knowledge, the literature contains only one similar report that examines and attempts to correlate H_2 evolution with pH evolution in the context of aluminium hydrolysis [48]. This report also identifies and proposes the existence of distinct reaction phases or zones, each exhibiting unique effects on pH level.

At 0.5 M NaOH and 1 M the pH rises instead of fall (Fig. 9). This fits a model with no zone, or time with dissolution without precipitation. Moreover, the rise in pH is more rapid than can be modelled by the theoretical increase in [OH-] as predicted by reaction R1, namely 3 mol of [OH-] generated per mole of Al^{3+} alone – the model R1 line in Figs. 9 and 10 underestimates the increase in pH if it is implemented strictly.

Two possible explanations that would fit the data well is illustrated by the models R1* plotted in Figs. 9 and 10. The R1* model can be achieved in two equivalent ways. Firstly, if 4.5 [OH-] ions are released per Al hydrolysed (per $1.5H_2$ evolved) that would change the R1 model to the R1* curve that closely fits the data. The second explanation is that the dissolution of metal into the electrolyte also changes the hydroxide activity coefficient. At 0.5 M this change would be from the measured value of $\gamma_{OH^-} = 1.06$ prior to metal introduction, to a value of $\gamma_{OH^-} = 1.6$ after metal introduction.

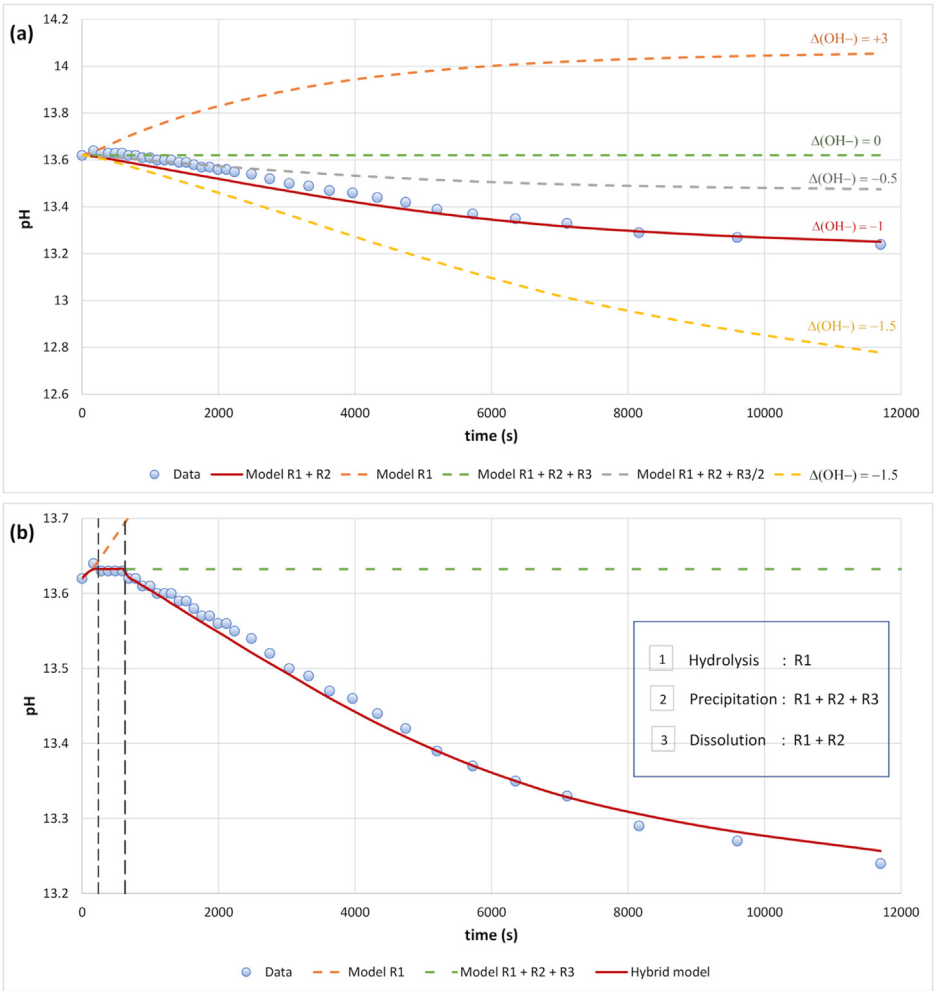

Fig. 8 – (a) Best fit model for pH at 0.24 M NaOH (ΔOH- represents the change in the amount of hydroxide ions) and (b) measured pH and H_2 model for pH at 0.24 M NaOH.

Please cite this article as: Urbonavicius M et al., Hydrogen from industrial aluminium scraps: Hydrolysis under various conditions, modelling of pH behaviour and analysis of reaction by-product, International Journal of Hydrogen Energy, https://doi.org/10.1016/j.ijhydene.2023.09.065

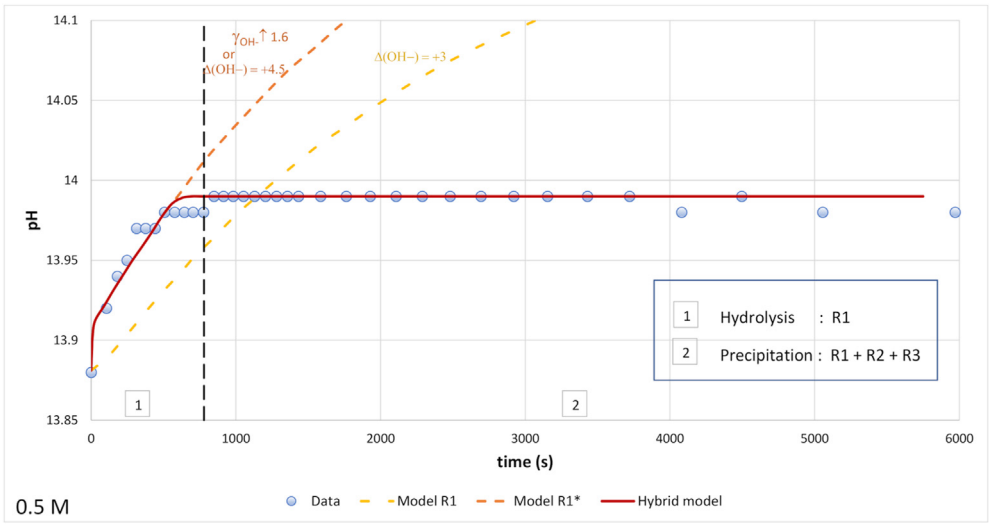

Fig. 9 – Measured pH and H_2 model for pH at 0.5 M NaOH.

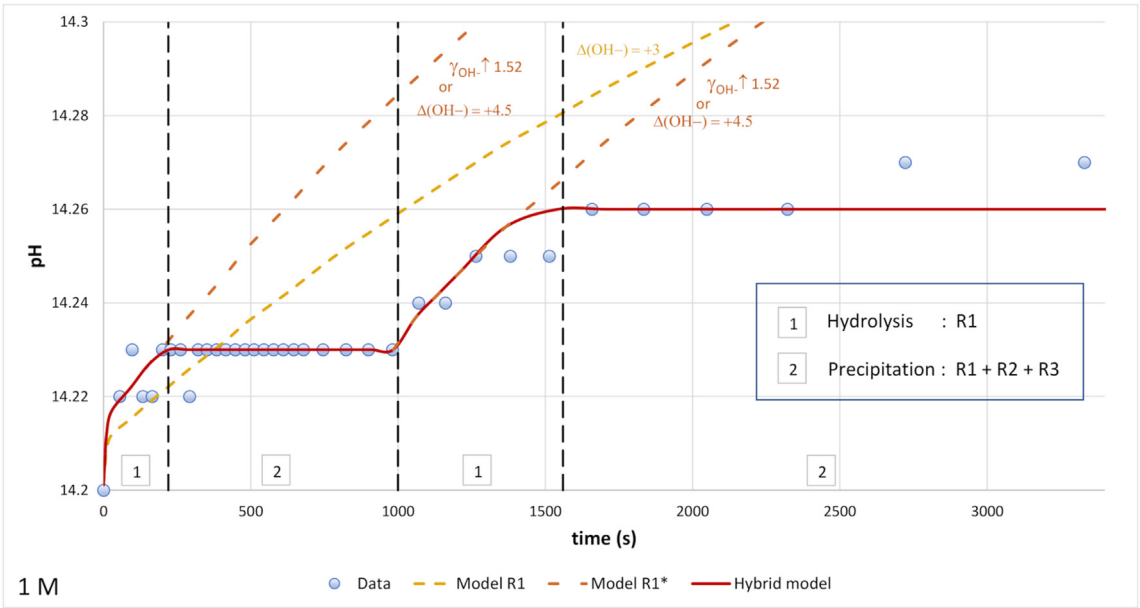

Fig. 10 – Measured pH and H_2 model for pH at 1 M NaOH.

In both the 0.5 M NaOH and 1 M NaOH data, an increase in the activity coefficient by a factor of 1.5 produces the R1* model curves that closely fit the measured pH data and correlates the measured H_2 to the pH change. In the absence of any apparent chemistry that could result in a net increase of 4.5 mol [OH-] per mole Al hydrolysed, perhaps the most parsimonious conjecture is that an upshift in hydroxide activity occurs as metal ions dissolve into the electrolyte. The resulting trends for activity coefficient change, and the magnitude thereof, is within typical values of γ_{OH^-} reported in other studies [55,56]. In particular, Christov et al. [56] measured γ_{OH^-} values that at low pH first decrease below 1 as alkalinity increase, but then at higher even higher alkalinity γ_{OH^-} as a function of [OH-] curve back upwards and achieve values with $\gamma_{OH^-} > 1$ up to the ranges suggested here. Delegard et al. [55] suggested that in addition to just NaOH or base molarity, the addition of other anions or cations (like Al3+) can also significantly alter γ_{OH^-}.

It is worth noting that since the pH only directly measures the product of γ_{OH^-} and [OH-]. Therefore, it is impossible to establish empirically, or definitively, to what degree the observed increase in pH here is due to an increase in γ_{OH^-} or [OH-] from a pH measurement alone. In Fig. 9, the model R1*, that fits the data well, is the result of postulating the release of 3 [OH-] ions per Al^{3+} ion (i.e., 3 [OH-] ions per 1.5H_2 measured in the experiment) and then also assuming that the activity coefficient γ_{OH^-} increases from 1.06 to 1.6 upon the metal ion generation. However, mathematically, the pH model yields identical results when assuming a fixed activity coefficient (γ_{OH^-}) at its pre-metal value of 1.06, and instead assuming reactions that increase the number of hydroxide ions by approximately 4.5 mol for every mole of Al^{3+}. These are two

Please cite this article as: Urbonavicius M et al., Hydrogen from industrial aluminium scraps: Hydrolysis under various conditions, modelling of pH behaviour and analysis of reaction by-product, International Journal of Hydrogen Energy, https://doi.org/10.1016/j.ijhydene.2023.09.065

examples belonging to a family of models that result the same product of γ_{OH^-} and [OH-]. Both models, referred to as "model R1*", demonstrate a good fit to the measured pH data shown in Fig. 9 until the point where the "precipitation phase" begins and the pH levels off.

Fig. 10 shows the measured pH evolution vs time at 1 M. The same trend as at 0.5 M (Fig. 9) is repeated, with a rapid increase in pH (as predicted by R1), followed by a levelling off of pH (as predicted by R1+R2+R3). However, at 1000 s, a similar pattern emerges – an upshift in pH followed by stabilization, even though the evolution of H_2 continues.

Exactly as in Fig. 9, the data can be most accurately fitted if the hydroxide activity γ_{OH^-} increases by a factor of approximately 1.5 after the introduction of metal. In the case of 1 M NaOH, γ_{OH^-} increases from an initial measured pre-metal value of 1.01 to a best fit value of 1.52 after the introduction of the metal.

The observed trend in this experiment, wherein the pH stabilized for about 780 s (from 220 s to 1000 s), followed by a subsequent drift upwards and another stabilization around 1560 s, is evidently complex. In a second run similar behaviour is observed with the exact time points for stabilization potentially varying from run to run. This somewhat indetermined complexity in the pH measurement of Al metal ion solutions is consistent with the findings of several early studies investigating the nature of aluminium solubility, like Hem & Roberson [57] or Rubin & Hayden [58] who did detailed investigations of the nature of Al ions in solution, and the reputed "polymerization" of ions like $Al(OH)_4^-$ polymeric networks. Their work suggests that Al ions, particularly the $Al(OH)_4^-$ ion, which is the predominant Al ion under the alkaline conditions studied here, have the potential to self-organize into polymeric networks over time. These networks may eventually lead to the formation of hydroxide gel or correspond to the crystal structure observed during hydroxide precipitation. Regarding the somewhat complex dynamics of this polymerization process and its relation to "the effects of [Al ion complex] polymerization on pH during aging", Hem & Roberson noted that while the solution or precipitation of aluminium hydroxide is often simplified as a chemical equilibrium, a more likely representation involves a complex reaction scheme with both slow and fast steps. And in general, they described a somewhat complex, and possibly partially quasi-chaotic or indeterminate evolution of the pH with Al dissolution. This evolution, as suggested by Hem & Roberson and previous researchers, is predominantly linked to anion complex polymerization during the aging. For instance, Hem & Roberson observed greater pH measurement uncertainty, particularly at lower pH levels, detailed in the "Factors controlling pH" section [57]. Due to the significant presence of structural OH in polymerized species, a direct connection between pH and degree of polymerization could not be established. For example, a pH of 4.43 appeared when over half of aluminium slowly polymerized, matching pH when only 15% polymerized. Authors explained that growing polymeric aggregates lower pH as protons transfers from water molecules within the octahedra $[[Al^{3+}(H20)_{6-x}(OH\text{-})_x^{-(x-3)}]$, eventually entering the solution due to all Al octahedra internal spots occupied by [OH-] ions. Qualitative observation of the impact of polymeric species on solution pH was evident in multiple experiments.

Upon the aforementioned observations, it is essential to examine the XRD results of the reaction by-product, which provide further insights. The XRD results of the reaction by-product using various alkali concentrations (0.24, 0.5, and 1 M) are presented in Fig. 11. The reaction by-product was analysed at different stages: (1) the precipitated by-product that was dried after the reaction was completely finished, and (2) the reaction by-product dried and washed with distilled water.

Before the measurement at step (1), the by-product was removed from the alkali and dried under ambient conditions. Normally, Al-water reaction at room temperature results in the formation of the $Al(OH)_3$ by-product. However, in this case, the (1) diffractogram mainly consisted of thermonatrite ($Na_2(CO_3)H_2O$, JCPDS: 01-070-2148), small peaks of $Al(OH)_3$ (JCPDS: 00-020-0011), and very tiny peaks of sodium oxide hydrate ($Na_2(O_2)(H_2O)_8$, JCPDS: 04-011-1675). Thermonatrite is typically formed by the reaction of CO_2 with NaOH, and it is well known that NaOH solution can be used as an absorbent to capture CO_2 [53]. In this case, it is possible that the wet by-product may have absorbed CO_2 during the removal and drying process due to the prolonged contact with air as shown in the following equation (9).

$$2NaOH_{(aq)} + CO_{2(g)} \rightarrow Na_2CO_{3(aq)} + H_2O_{(l)} \quad (9)$$

Since thermonatrite is water-soluble, it was easily washed out by rinsing the by-product with distilled water. Thus, only the $Al(OH)_3$ phase was identified in all cases of alkali solution in the (2) spectra of Fig. 11. The crystallite sizes of the washed by-product of 0.24, 0.5, and 1 M were found to be 32.6, 36.2, and 28.4 nm, respectively, indicating the synthesis of nanocrystalline product.

The aluminium hydroxide by-product can be used as a precursor to produce gamma alumina, which is formed at temperatures above 500 °C [59] and can be used as a valuable industrial product [60,61] or fed back into the aluminium production process.

The measurement results of BET-specific surface area for the by-product samples (Table 1) indicated that the samples containing sodium carbonate as the primary phase have significantly lower BET values, typically ranging from 1 to 3 m^2/g (occasionally slightly above 20 m^2/g). In contrast, samples consisting solely of aluminium hydroxide exhibited a specific surface area within the expected range of approximately 220 m^2/g.

The low BET surface area of samples can be attributed to contamination with NaOH, as mentioned above, during the drying process. It is worth noting that this reaction can also occur with solid NaOH that contains moisture. Hence, it is crucial to take caution when preparing a sodium hydroxide solution to avoid such contamination.

Please cite this article as: Urbonavicius M et al., Hydrogen from industrial aluminium scraps: Hydrolysis under various conditions, modelling of pH behaviour and analysis of reaction by-product, International Journal of Hydrogen Energy, https://doi.org/10.1016/j.ijhydene.2023.09.065

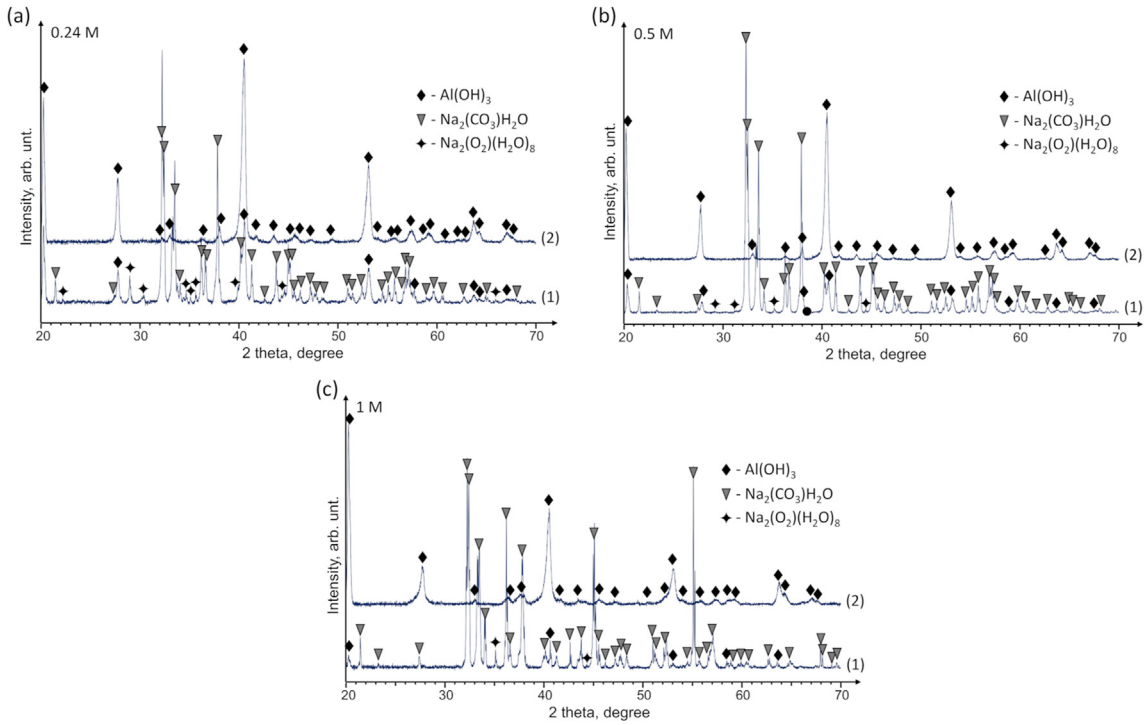

Fig. 11 – XRD patterns of the by-product after the reaction of aluminium with water at different NaOH molarities. The spectra include: (1) the pattern of dried reaction by-product obtained after the completion of the reaction, and (2) the pattern of washed reaction by-product. The molarities of NaOH used were (a) 0.24 M, (b) 0.5 M, and (c) 1 M.

Table 1 – The BET-specific surface area of samples.

Molarity of reaction solution	BET surface area of by-products, m^2/g	
	Before wash	After wash
0.24 M	12.6	≈220
0.5 M	2.9	≈220
1 M	1.2	≈220

4. Conclusions

The Al-water reaction and its kinetics can be influenced by several factors: temperature, alkali concentration, water amount, aluminium mass, and its ratio with alkali concentration, and even heat dissipated during the reaction. In particular, temperature plays an important role in the reaction kinetics, and proper thermal insulation of the vessel can even promote the hydrogen production process due to the heat dissipated in the exothermic reaction. The results presented in this work showed that even with a relatively low alkali concentration, relatively intensive H_2 yield can be reached by optimizing and raising the initial reaction temperature, the amount of waste aluminium scrap, or insulation of reaction vessel (i.e. using self-heating in the adiabatic reactor). The Arrhenius equation accurately fitted the measured data and allowed the estimation of the activation energy as 48.1 kJ/mol when using only a 0.24 M alkali solution. The experiment revealed that the pH behaviour during aluminium dissolution is complex and does not follow a straightforward pattern. The oversight of temperature and atmospheric air exposure in the initial experiment was addressed by conducting new experiments in an isothermal environment. The pH decreased at a concentration of 0.24 M NaOH, while at higher concentrations of 0.5 M and 1 M NaOH, the pH either increased or remained relatively constant despite significant hydrogen evolution. The increase in pH at higher NaOH concentrations could be explained by an upshift in the hydroxide activity coefficient. The 0.24 M modelling suggests that the reaction passes through three zones: hydrolysis, precipitation, and dissolution. Meanwhile, the 0.5 M and 1 M concentrations indicate two zones: hydrolysis and precipitation. The complex pH evolution suggests the involvement of polymerization processes and the formation of polymeric networks of aluminium ions.

Further analysis revealed that the by-product obtained from the alkali solution and dried under ambient conditions contains a substantial amount of thermonatrite, which results in a relatively low surface area (1–2 m^2/g). Therefore, an additional step is required, namely rinsing the by-product with distilled water, to avoid contamination and improve

Please cite this article as: Urbonavicius M et al., Hydrogen from industrial aluminium scraps: Hydrolysis under various conditions, modelling of pH behaviour and analysis of reaction by-product, International Journal of Hydrogen Energy, https://doi.org/10.1016/j.ijhydene.2023.09.065

surface area to approximately 220 m^2/g. It is essential to use CO_2-free NaOH when producing $Al(OH)_3$ by reacting aluminium with sodium hydroxide. It is also important to prevent CO_2 from entering the reactor. If that is done, it is possible to produce high surface area alumina from $Al(OH)_3$ obtained by reacting aluminium with NaOH solution.

Investigated Al water reaction has high potential for clean hydrogen and energy production, but the feasibility of the recycling process and proper scaling will require a proper combination of kinetics influencing parameters. We must consider the hazardous nature of high concentration alkali solutions and environmental and economic implications. Further investigation of full cycle influence on the economic and environmental influence of such recycling process has to be done in addition to other electrolyte compositions.

Funding

This research is funded by the Baltic Research Programme project No. EEA-RESEARCH-92 "Aluminum in circle economy - from waste through hydrogen energy to alumina" – AliCE-Why" under the EEA Grant of Iceland, Liechtenstein and Norway (No. EEZ/BPP/VIAA/2021/5).

Declaration of competing interest

The authors declare that they have no known competing financial interests or personal relationships that could have appeared to influence the work reported in this paper.

Acknowledgments

EU CAMART2 project (European Union's Horizon 2020 Framework Programme H2020-WIDESPREAD-01-2016-2017-TeamingPhase2 under grant agreement No. 739508).

REFERENCES

[1] Varjani S, Shahbeig H, Popat K, Patel Z, Vyas S, Shah AV, et al. Sustainable management of municipal solid waste through waste-to-energy technologies. Bioresour Technol 2022;355:127247. https://doi.org/10.1016/j.biortech.2022.127247.

[2] Andeobu L, Wibowo S, Grandhi S. An assessment of e-waste generation and environmental management of selected countries in Africa, Europe and North America: a systematic review. Sci Total Environ 2021;792:148078. https://doi.org/10.1016/j.scitotenv.2021.148078.

[3] Kaza S, Yao L, Bhada-Tata P, Van Woerden F. What a waste 2.0: a global snapshot of solid waste management to 2050. The World Bank; 2018. https://doi.org/10.1596/978-1-4648-1329-0.

[4] Wijayasekera SC, Hewage K, Hettiaratchi P, Siddiqui O, Razi F, Pokhrel D, et al. Sustainability of waste-to-hydrogen conversion pathways: a life cycle thinking-based assessment. Energy Convers Manag 2022;270:116218. https://doi.org/10.1016/j.enconman.2022.116218.

[5] Pi X, Fei X, Wang Y, Sun X, Guo Y. Global void ratio of municipal solid waste for compression indices estimation. Waste Manag 2023;160:69–79. https://doi.org/10.1016/j.wasman.2023.02.003.

[6] Vyas S, Prajapati P, Shah AV, Varjani S. Municipal solid waste management : dynamics , risk assessment , ecological in fl uence , advancements , constraints and perspectives. Sci Total Environ 2022;814:152802. https://doi.org/10.1016/j.scitotenv.2021.152802.

[7] Wu S, Montalvo L. Repurposing waste plastics into cleaner asphalt pavement materials : a critical literature review. J Clean Prod 2021;280:124355. https://doi.org/10.1016/j.jclepro.2020.124355.

[8] Anuardo RG, Espuny M, Carolina A, Costa F. Toward a cleaner and more sustainable world : a framework to develop and improve waste management through organizations , governments. Heliyon 2022;8. https://doi.org/10.1016/j.heliyon.2022.e09225.

[9] European Aluminium Association. A strategy for achieving aluminium'S full potential for circular economy by 2030. 2020.

[10] Raabe D, Ponge D, Uggowitzer PJ, Roscher M, Paolantonio M, Liu C, et al. Making sustainable aluminum by recycling scrap: the science of "dirty" alloys. Prog Mater Sci 2022;128:100947. https://doi.org/10.1016/j.pmatsci.2022.100947.

[11] Lepage T, Kammoun M, Schmetz Q, Richel A. Biomass-to-hydrogen: a review of main routes production, processes evaluation and techno-economical assessment. Biomass Bioenergy 2021;144:105920. https://doi.org/10.1016/j.biombioe.2020.105920.

[12] Tekade SP, Jadhav GR, Kalekar SE, Pednekar AS, Shende DZ, Wasewar KL, et al. Utilization of human urine and waste aluminum for generation of hydrogen. Bioresour Technol Rep 2021;15:100821. https://doi.org/10.1016/j.biteb.2021.100821.

[13] Srivastava A, Meshram A. On trending technologies of aluminium dross recycling : a review. Process Saf Environ Protect 2023;171:38–54. https://doi.org/10.1016/j.psep.2023.01.010.

[14] Trowell KA, Goroshin S, Frost DL, Bergthorson JM. Aluminum and its role as a recyclable, sustainable carrier of renewable energy. Appl Energy 2020;275:115112. https://doi.org/10.1016/j.apenergy.2020.115112.

[15] Xiao F, Yang R, Liu Z. Active aluminum composites and their hydrogen generation via hydrolysis reaction: a review. Int J Hydrogen Energy 2022;47:365–86. https://doi.org/10.1016/j.ijhydene.2021.09.241.

[16] Tekade SP, Pednekar AS, Jadhav GR, Kalekar SE, Shende DZ, Wasewar KL. Hydrogen generation through water splitting reaction using waste aluminum in presence of gallium. Int J Hydrogen Energy 2020;45:23954–65. https://doi.org/10.1016/j.ijhydene.2019.09.026.

[17] Brayek M, Jemni MA, Driss Z, Kantchev G, Abid MS. Study of spark-ignition engine fueled with hydrogen produced by the reaction between aluminum and water in presence of KOH. Arabian J Sci Eng 2019;44:695–705. https://doi.org/10.1007/s13369-018-3192-4.

[18] Abánades A. Natural gas decarbonization as tool for greenhouse gases emission control. Front Energy Res 2018;6:1–7. https://doi.org/10.3389/fenrg.2018.00047.

[19] Fiorio JL, Gothe ML, Kohlrausch EC, Zardo ML, Tanaka AA, de Lima RB, et al. Nanoengineering of catalysts for enhanced hydrogen production. Hydrogen 2022;3:218–54. https://doi.org/10.3390/hydrogen3020014.

[20] Pistidda C. Solid-state hydrogen storage for a decarbonized society. Hydrogen 2021;2:428–43. https://doi.org/10.3390/hydrogen2040024.

Please cite this article as: Urbonavicius M et al., Hydrogen from industrial aluminium scraps: Hydrolysis under various conditions, modelling of pH behaviour and analysis of reaction by-product, International Journal of Hydrogen Energy, https://doi.org/10.1016/j.ijhydene.2023.09.065

[21] Wang H, Chung H, Teng H, Cao G. Generation of hydrogen from aluminum and water - effect of metal oxide nanocrystals and water quality. Int J Hydrogen Energy 2011;36:15136–44. https://doi.org/10.1016/j.ijhydene.2011.08.077.
[22] Gany A, Elitzur S, Rosenband V. Compact Electric Energy Storage for Marine Vehicles Using on-Board Hydrogen Production. 2015. p. 151–8. https://doi.org/10.17265/2159-5879/2015.04.001. 5.
[23] Haller MY, Carbonell D, Dudita M, Zenhäusern D, Häberle A. Seasonal energy storage in aluminium for 100 percent solar heat and electricity supply. Energy Convers Manag X 2020;5:100017. https://doi.org/10.1016/j.ecmx.2019.100017.
[24] Kim M, Eom K, Kwon J, Cho E, Kwon H. On-board hydrogen production by hydrolysis from designed Al-Cu alloys and the application of this technology to polymer electrolyte membrane fuel cells. J Power Sources 2012;217:345–50. https://doi.org/10.1016/j.jpowsour.2012.06.008.
[25] Guo J, Su Z, Tian J, Deng J, Fu T, Liu Y. Enhanced hydrogen generation from Al-water reaction mediated by metal salts. Int J Hydrogen Energy 2021;46:3453–63. https://doi.org/10.1016/j.ijhydene.2020.10.220.
[26] Oliveira AM, Beswick RR, Yan Y. A green hydrogen economy for a renewable energy society. Curr Opin Chem Eng 2021;33:100701. https://doi.org/10.1016/j.coche.2021.100701.
[27] Abe JO, Popoola API, Ajenifuja E, Popoola OM. Hydrogen energy, economy and storage: review and recommendation. Int J Hydrogen Energy 2019;44:15072–86. https://doi.org/10.1016/j.ijhydene.2019.04.068.
[28] Ho CY, Huang CH. Enhancement of hydrogen generation using waste aluminum cans hydrolysis in low alkaline de-ionized water. Int J Hydrogen Energy 2016;41:3741–7. https://doi.org/10.1016/j.ijhydene.2015.11.083.
[29] Lim ST, Sethupathi S, Alsultan AG, Munusamy Y. Hydrogen production via activated waste aluminum cans and its potential for methanation. Energy Fuel 2021;35:16212–21. https://doi.org/10.1021/acs.energyfuels.1c02277.
[30] Salueña-Berna X, Marín-Genescà M, Massagués Vidal L, Dagà-Monmany JM. Waste aluminum application as energy valorization for hydrogen fuel cells for mobile low power machines applications. Materials 2021;14:7323. https://doi.org/10.3390/ma14237323.
[31] Liu Y, Wang X, Liu H, Dong Z, Li S, Ge H, et al. Improved hydrogen generation from the hydrolysis of aluminum ball milled with hydride. Energy 2014;72:421–6. https://doi.org/10.1016/j.energy.2014.05.060.
[32] Zhang F, Edalati K, Arita M, Horita Z. Fast hydrolysis and hydrogen generation on Al-Bi alloys and Al-Bi-C composites synthesized by high-pressure torsion. Int J Hydrogen Energy 2017;42:29121–30. https://doi.org/10.1016/j.ijhydene.2017.10.057.
[33] Yang B, Zhu J, Jiang T, Gou Y, Hou X, Pan B. Effect of heat treatment on Al–Mg–Ga–In–Sn alloy for hydrogen generation through hydrolysis reaction. Int J Hydrogen Energy 2017;42:24393–403. https://doi.org/10.1016/j.ijhydene.2017.07.091.
[34] Yang W, Zhang T, Zhou J, Shi W, Liu J, Cen K. Experimental study on the effect of low melting point metal additives on hydrogen production in the aluminum-water reaction. Energy 2015;88:537–43. https://doi.org/10.1016/j.energy.2015.05.069.
[35] Chai YJ, Dong YM, Meng HX, Jia YY, Shen J, Huang YM, et al. Hydrogen generation by aluminum corrosion in cobalt (II) chloride and nickel (II) chloride aqueous solution. Energy 2014;68:204–9. https://doi.org/10.1016/j.energy.2014.03.011.
[36] Meng A, Sun Y, Cheng W, Zhai Z, Jiang L, Chong Z, et al. Mechanism of hydrogen generation from low melting point elements (Ga, In, Sn) on aluminum alloy hydrolysis. Int J Hydrogen Energy 2022;47:39364–75. https://doi.org/10.1016/j.ijhydene.2022.09.127.
[37] du Preez SP, Bessarabov DG. On-demand hydrogen generation by the hydrolysis of ball-milled aluminum composites: a process overview. Int J Hydrogen Energy 2021;46:35790–813. https://doi.org/10.1016/j.ijhydene.2021.03.240.
[38] Levenspiel O. Chemical reaction engineering. 3rd ed. John Wiley & Sons, Inc.; 1999.
[39] Elitzur S, Rosenband V, Gany A. Study of hydrogen production and storage based on aluminum-water reaction. Int J Hydrogen Energy 2014;39:6328–34. https://doi.org/10.1016/j.ijhydene.2014.02.037.
[40] Huang X, Gao T, Pan X, Wei D, Lv C, Qin L, et al. A review : feasibility of hydrogen generation from the reaction between aluminum and water for fuel cell applications. J Power Sources 2013;229:133–40. https://doi.org/10.1016/j.jpowsour.2012.12.016.
[41] Shkolnikov EI, Zhuk AZ, Vlaskin MS. Aluminum as energy carrier : feasibility analysis and current technologies overview. Renew Sustain Energy Rev 2011;15:4611–23. https://doi.org/10.1016/j.rser.2011.07.091.
[42] Baes CF, Mesmer RS. The hydrolysis of cations. John Wiley & Sons, Inc.; 1976.
[43] Haller MY, Amstad D, Dudita M, Englert A, Häberle A. Combined heat and power production based on renewable aluminium-water reaction. Renew Energy 2021;174:879–93. https://doi.org/10.1016/j.renene.2021.04.104.
[44] Kader MS, Zeng W, Johnston E, Buckner SW, Jelliss PA. A novel method for generating H2 by activation of the μAl-water system using aluminum nanoparticles. Appl Sci 2022;12:5378. https://doi.org/10.3390/app12115378.
[45] Kanehira S, Kanamori S, Nagashima K, Saeki T, Visbal H, Fukui T, et al. Controllable hydrogen release via aluminum powder corrosion in calcium hydroxide solutions. J Asian Ceram Soc 2013;1:296–303. https://doi.org/10.1016/j.jascer.2013.08.001.
[46] Xiao F, Zhang B, Lee C. Effects of low temperature on aluminum(III) hydrolysis: theoretical and experimental studies. J Environ Sci 2008;20:907–14. https://doi.org/10.1016/S1001-0742(08)62185-3.
[47] Soler L, Macanas J, Munoz M, Casado J. Aluminum and aluminum alloys as sources of hydrogen for fuel cell applications. J Power Sources 2007;169:144–9. https://doi.org/10.1016/j.jpowsour.2007.01.080.
[48] Kanehira S, Kanamori S, Nagashima K, Saeki T, Visbal H, Fukui T, et al. Controllable hydrogen release via aluminum powder corrosion in calcium hydroxide solutions. J Asian Ceram Soc 2013;1:296–303. https://doi.org/10.1016/j.jascer.2013.08.001.
[49] Curioni M, Scenini F. The mechanism of hydrogen evolution during anodic polarization of aluminium. Electrochim Acta 2015;180:712–21. https://doi.org/10.1016/j.electacta.2015.08.076.
[50] Wang C, Yang T, Liu Y, Ruan J, Yang S, Liu X. Hydrogen generation by the hydrolysis of magnesium-aluminum-iron material in aqueous solutions. Int J Hydrogen Energy 2014;39:10843–52. https://doi.org/10.1016/j.ijhydene.2014.05.047.
[51] Gai W-Z, Wang L-Y, Lu M-Y, Deng Z-Y. Effect of low concentration hydroxides on Al hydrolysis for hydrogen production. Energy 2023;268:126731. https://doi.org/10.1016/j.energy.2023.126731.
[52] Wefers K, Misra C. Oxides and hydroxides of aluminum. Alcoa Research Laboratories; 1987.
[53] Yoo M, Han S-J, Wee J-H. Carbon dioxide capture capacity of sodium hydroxide aqueous solution. J Environ Manag

Please cite this article as: Urbonavicius M et al., Hydrogen from industrial aluminium scraps: Hydrolysis under various conditions, modelling of pH behaviour and analysis of reaction by-product, International Journal of Hydrogen Energy, https://doi.org/10.1016/j.ijhydene.2023.09.065

2013;114:512–9. https://doi.org/10.1016/j.jenvman.2012.10.061.
[54] Shilov IY, Lyashchenko AK. Activity coefficient modeling for aqueous aluminum salt solutions in terms of the generalized Debye–Hückel theory. Russ J Inorg Chem 2019;64:1186–9. https://doi.org/10.1134/S0036023619090213.
[55] Delegard C, Pearce C, Dembowski M, Snyder M, Leavy I, Baum S, et al. Aluminum hydroxide solubility in sodium hydroxide solutions containing nitrite/nitrate of relevance to hanford tank waste. 2018. https://doi.org/10.2172/1660940.
[56] Christov C, Moller N. Chemical equilibrium model of solution behavior and solubility in the H-Na-K-OH-Cl-HSO4-SO4-H2O system to high concentration and temperature. Geochem Cosmochim Acta 2004;68:1309–31. https://doi.org/10.1016/j.gca.2003.08.017.
[57] Hem JD, Roberson CE. Form and stability of aluminum hydroxide complexes in dilute solution. 1967. https://doi.org/10.3133/wsp1827A.
[58] Rubin AJ, Hayden PL. Studies on the hydrolysis and precipitation of aluminum(III). 1973.
[59] Urbonavicius M, Varnagiris S, Pranevicius L, Milcius D. Production of gamma alumina using plasma-treated aluminum and water reaction byproducts. Materials 2020;13:1–12. https://doi.org/10.3390/ma13061300.
[60] Ali S, Abbas Y, Zuhra Z, Butler IS. Synthesis of γ-alumina (Al2O3) nanoparticles and their potential for use as an adsorbent in the removal of methylene blue dye from industrial wastewater. Nanoscale Adv 2019;1:213–8. https://doi.org/10.1039/c8na00014j.
[61] Razm AH, Salem A, Salem S. Industrial performance, reusability and mechanical reliability of mesoporous gamma alumina packed bed fabricated through boehmite extrusion for removal of reactive dyes from textile wastewaters. J Hazard Mater 2022;429:128259. https://doi.org/10.1016/j.jhazmat.2022.128259.

Please cite this article as: Urbonavicius M et al., Hydrogen from industrial aluminium scraps: Hydrolysis under various conditions, modelling of pH behaviour and analysis of reaction by-product, International Journal of Hydrogen Energy, https://doi.org/10.1016/j.ijhydene.2023.09.065